Calibration of the Stark-broadening parameters for some He I lines

C. Pérez, I. de la Rosa, A. M. de Frutos, and S. Mar
Departamento de Física Aplicada III, Facultad de Ciencias (Universidad de Valladolid), 47071 Valladolid, Spain
(Received 17 January 1991; revised manuscript received 3 June 1991)

The Stark broadening of several He I lines has been measured in a pulsed arc plasma. The intensity ratio of the He II (4686 Å) and the He I (6678 Å) lines was used to estimate the electron temperature, while the electron density was independently determined from interferometry at five different wavelengths. The electron density of the plasma varies from $(2.00–6.46)\times10^{16}$ cm^{-3} and the temperature from 19 000 to 43 000 K. The results of this work are compared with the available experimental data, and all of them are used to calibrate some He I lines, which will be used as calibration lines in future work with more complex plasmas.

PACS number(s): 52.70.Kz, 32.60.+i

I. INTRODUCTION

Stark broadening of helium spectral lines is of great interest in plasma diagnostics, in laboratory as well as in stellar plasmas. Since helium is used as carrier gas in many laboratory plasmas, it would be very useful to have calibrated helium lines in order to solve the problem of plasma diagnostics. In this work, three isolated He I lines of 5016 Å ($2\,^1S-3\,^1P°$), 4713 Å ($2^3P°-4\,^3S$), and 6678 Å ($2\,^1P°-3\,^1D$) have been calibrated. To carry on these calibrations, we have done independent determinations of the plasma electron density, temperature, and full halfwidths of the lines.

For the He I line at 5016 Å, a wide bibliography of previous experiments exists, and the results from them are, in general, in good agreement with the theoretical values by Griem [1] and Dimitrijevic and Sahal-Brechot [2]. But for the other two lines, there are very few previous experimental data, and, the agreement with the theory is not as good, especially for electron densities above 10^{17} cm^{-3}.

II. EXPERIMENTAL SETUP AND PLASMA DIAGNOSTICS

A. Plasma source and experimental arrangement

The plasma source used in this experiment is a pulsed arc. The lamp consists of a cylinder made of Pyrex glass with 15 cm length and 2 cm inner diameter. Two annular pieces made of aluminum that are glued to the ends of the tube are the electrodes. On the walls of these electrodes there are two O-rings and on them, there are the glass windows of the lamp. The length of the Pyrex tube exceeds the electrodes; this is done in order to protect, as much as possible, the areas near the electrodes, avoiding that the materials coming from them during the discharge could reach the measurement zone. The electrical wires are attached symmetrically to the electrodes to avoid inhomogeneities in the plasma. The lamp is also connected to vacuum and gas systems by standard connections situated on the electrodes. The excitation unit, that has been designed and constructed in this laboratory, is described elsewhere [3].

In this work, spectroscopic and interferometric measurements have been done. The whole experimental setup is in Fig. 1. The lamp is placed in one of the arms of a Twyman-Green interferometer. The arms of this interferometer are formed with the mirrors M_1 and M_2 and the beam splitter BS_1. Another beam splitter BS_2, located on the interferometer exit arm, splits the light from the lamp into two beams, which are directed to the spectroscopic and the interferometric channels, respectively.

The latter goes into a microscope objective, MO, that focuses it onto the entrance slit of a monochromator which is tuned to the working wavelength, to eliminate the lamp flash. At the exit slit, the light is detected by a photomultiplier PM_1 that sends the signal to a digital oscilloscope, and from there to the computer. The temporal resolution of the interferometric measurements was 0.2 μs.

The other beam is sent to the spectroscopic channel. All the measurements are end-on. The diaphragms D_1 and D_2 select a very narrow light beam which is focused, by the cylindrical lens, CL, onto the entrance slit of a Jobin-Yvon spectrometer with two concave spherical mirrors of 1500 mm of focal length and a grating of 1200 lines/mm. The spectra are recorded by the detector (vidicon) at the exit plane of the spectrometer, and they are sent from there to an optical multichannel analyzer (OMA). The pulse that polarizes the vidicon comes from a pulses generator that gives pulses whose amplitude, width, and delay can be selected. The plasmas created in these experiments last, on the average, about 100 μs, and the width of the polarization pulses is 5 μs, so that our spectra can be considered as instantaneous and it is possible to follow the plasma temporal evolution.

The pulse generator is triggered by the signal emitted by the photomultiplier, PM_2, when it receives the lamp light. On the oscilloscope the luminous signal and the polarization pulse are displayed simultaneously. In this way, we are sure that all the spectra are taken at the right moment. The same signal that triggers the spectroscopic channel activates the interferometric one.

Great care was taken to ensure that the profiles were

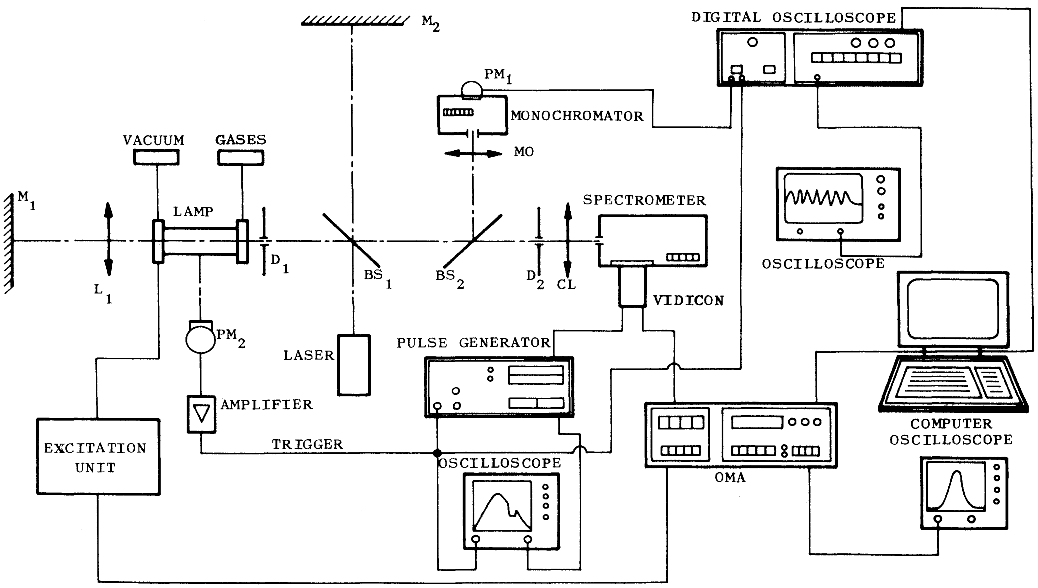

FIG. 1. Experimental arrangement.

not affected by self-absorption. This was achieved in the experimental arrangement with help of the lens, L_1 , and the flat mirror M_1. The lens forms the image of the lamp center onto itself, and in order to avoid the lens modifying the collimation of the beam in the interferometric arrangement, it is necessary that its focus lies on the mirror M_1.

B. Measurements and plasma diagnostics

During the whole experiment the lamp was working with a continuous flow of pure helium at a rate of 21 cm^3/min, a pressure of 11 mbar, and the plasma was created by discharging a capacitor bank of 20 μF charged to 9.2 kV. Under these experimental conditions the measured spectral lines have good intensities and negligible self-absorption.

The electron temperature was obtained from the intensities ratio of He II to He I lines. The lines from He II at 4686 Å and from He I 6678 Å were used. But, since it was impossible to get simultaneous measurements of He II and He I lines all over the plasma life, because the He II 4686-Å line is emitted only at very high temperatures (above 4 eV), and the determination of the plasma temperature with only He I lines is not very accurate due to the small values of the energy levels difference, an alternative method of determining temperatures in a pulsed plasma under local thermal equilibrium was developed [4], in order to be used in all cases in which the application of the conventional method is impossible. This method, which uses the total line intensities at interferometrically determined N_e, takes into account the local-thermodynamic-equilibrium (LTE) equations, using the known values of temperature as starting point; in this way, the method itself is a probe of the plasma LTE. Over the present work, this alternative method has been used in some instants of the plasma life, while in others we used the intensity ratio method. When possible, both methods have been applied simultaneously, in these cases there is a very good agreement between the results from both of them, as can be seen in Fig. 2.

The electron density was obtained by interferometry at several wavelengths [5]. The Twyman-Green interferometer worked at five different wavelengths, one of them from a He-Ne laser 6328 Å, and the rest from an Argon laser 4765, 5880, 4965, and 5145 Å. In this way, we have been able to know the contribution to the plasma refractivity of the bound electrons. It is broadly accepted that the contribution of these electrons is constant with the

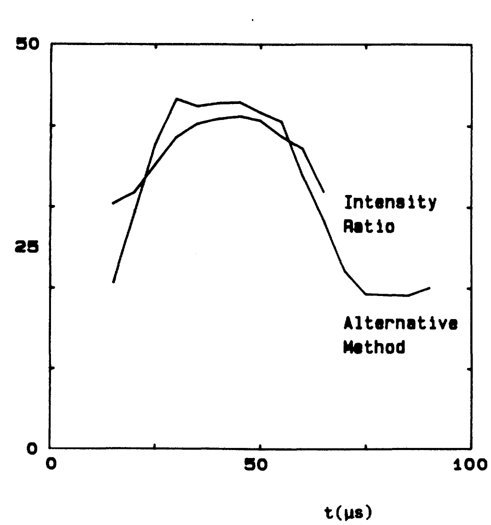

FIG. 2. Time evolution of the electron temperature obtained by two different methods.

wavelength, and this approximation is used to obtain the plasma refractivity from measurements at two wavelengths, or even at only one, assuming that this contribution is not only constant but also very small. But, as we have done these measurements at five wavelengths, we are able to determine this contribution. As a result, our interferometric measurements of the plasma electron density have a very high accuracy (better than 5%) and reliability. And also, we have to point out that the working wavelengths are far from the helium lines, so as not to have the possibility of anomalous dispersion near atomic resonances.

The computer processing of the interferometric records begins with the correction from the electrical and luminous background, the latter due to the lamp emission at the monochromator bandpass wavelength. Afterwards, we choose the phase origin. To do that, the final part of the interference pattern, when it has reached a stable state, was taken. The next step is the determination of the time at which the phase variation changes its sign. In every interferometric pattern it has been possible to find this moment. In this way, we determined a harmonic function of variable frequency. From this function we obtain the phase difference between the interference beams and the total plasma refractivity, from which we get the electron density.

The computer processing of the spectra has also different steps. As in the case of the interferometric patterns, in the first step, the background of electrical and luminous origin is eliminated. This leaves the spectral line and the continuum background. This continuum must be eliminated, so that it is necessary to know its structure. The basic processes responsible for it have different origins (recombination, bremsstrahlung), but according to Wiese [6], since the range of wavelengths is not very large, it is possible to assume this as $A+\lambda B$. But, A and B must be determined carefully, because the line parameters, in which we are interested (full halfwidth and intensity), depend very strongly on the choice of the continuum. The determination can be done in different ways [7], one of them is based on the fitting to the line wings, in the case of lines from nonhydrogenic elements, of a function like

$$A+B(\lambda-\lambda_C)+C(\lambda-\lambda_C)^{-2} ,$$

where λ_C refers to the line center. By a least-squares fitting to the wings (as far from the line center as possible, because the wings of the Lorentzian functions are very extended), it is possible to calculate the values of A and B, and also the value of C. These values allow us to obtain just the spectral line, i.e., its full width at half maximum (FWHM) and area. This area gives the total line intensity (used in temperature calculations) with the help of the transmittance of the whole system: monochromator, OMA, and vidicon, that we have previously measured [7].

To ensure that only the Stark broadening of the investigated lines was taken into account, all the profiles have been corrected for instrumental and Doppler broadening [8], even though these broadenings are almost negligible in most of the cases.

A last check of possible self-absorption in the measured lines is done. For that, as said above, there are measurements of the spectral lines with and without the mirror M_1. If we normalize the areas of two measurements (with and without the mirror) of the same spectral line taken at the same instant, they should have the same shape if there is no self-absorption, but if there is any we will see clear differences in the shapes of both measurements. After having done this check, it is possible to affirm that none of the spectral lines measured in this work had appreciable self-absorption.

III. RESULTS AND DISCUSSION

As already mentioned, for each of the measured lines, we obtained two series of data by independent determinations: the plasma electron densities and the full halfwidths. The measured values of these magnitudes are in Table I, w_m refers to the measured FWHM of the lines, the subscript 1 refers to the line at 6678 Å, 2 to 5016 Å, and 3 to 4713 Å. In this table the values of temperature have been also included.

As a first test of the consistency of our own results we have plotted, in Fig. 3, the pairs w_{m_1} vs w_{m_2}, w_{m_2} vs w_{m_3}, and w_{m_1} vs w_{m_3}. As it can be seen, there is a reasonably good linear fit in all of the three cases.

For each of the three lines, the FWHM has been plotted versus the electron density; this is done in Fig. 4. As predicted by theory, there is, in each case, a linear relationship between both sets of data.

We have also investigated the possible influence of the temperature in this dependence. Over the range of work temperatures (19 000–43 000 K), Fig. 5 shows for each line the ratio w_m/N_e vs T, the data present a large scatter, although it is possible to observe a tendency towards an increase of w_m/N_e with T for the 4713-Å line, and the inverse tendency for the other two lines (5016 and 6678 Å). These tendencies are in agreement with the theoretical predictions [1]. The question is whether this dependence of the experimental FWHM with the temperature is the same kind as predicted by theory [1]. There-

TABLE I. Experimental FWHM, electron densities and temperatures in the present work.

N_e (10^{16} cm^{-3})	w_1 (Å)	w_2 (Å)	w_3 (Å)	T (K)
6.46	4.24	4.40	6.67	36 450
6.26	4.07	3.96	6.22	40 950
5.56	3.92	3.98	5.51	41 350
5.15	3.78	3.78	5.05	41 850
4.88	3.55	3.72	4.41	42 050
4.51	3.27	3.42	4.66	41 100
4.01	2.83	2.97	4.06	39 600
3.59	2.62	2.64	3.62	35 550
3.23	2.31	2.37	2.95	30 150
2.88	2.27	2.11	2.66	22 100
2.59	2.26	2.00	2.17	19 200
2.35	2.02	1.89	2.05	19 100
2.00	1.75	1.76	1.78	19 000

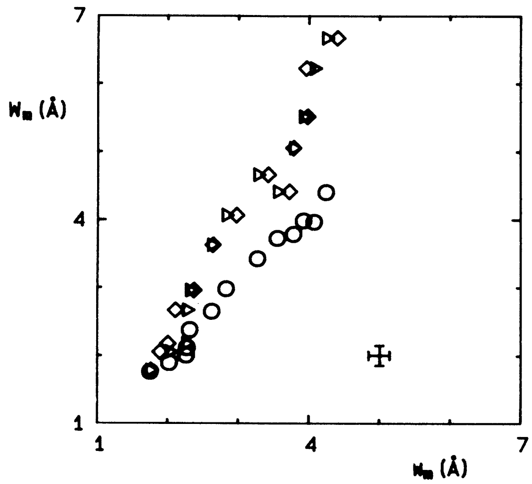

FIG. 3. FWHM vs FWHM for the three He I lines. ○, w_m (6678 Å) vs w_m (5016 Å); ◇, w_m (5016 Å) vs w_m (4713 Å); ▷, w_m (6678 Å) vs w_m (4713 Å). This figure includes the average error bars of the measurements obtained in the present work.

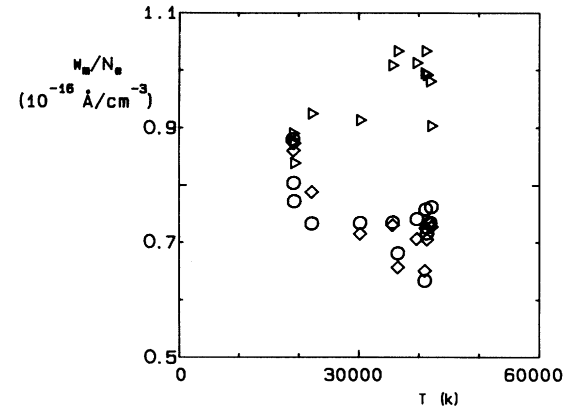

FIG. 5. Relative width (w_m/N_e) of the line as a function of the electron temperature. ◇, 6678 Å; ○, 5016 Å; and ▷, 4713 Å.

fore, we have plotted the ratio w_m/w_G (experimental to theoretical [1] FWHM) vs electron density in Fig. 6. From these figures, it is not possible to ascertain the existence of any clear relation of these ratios (w_m/w_G) with either electron density or temperature. For the 4713-Å line this quotient (w_m/w_G) is almost constant, for the other two lines, it is possible to notice a smooth trend, which may be due to the noise of our experimental data. The mean values of the calculated ratios (w_m/w_G) are the following: 0.85±0.08 for 6678 Å, 0.88±0.07 for 5016 Å, and 0.90±0.04 for 4713 Å.

In the next step, the results from this work are compared with previous data. Table II lists previous experimental data [9–18] for the 5016-Å He I line and the results from this work. The experimental full half-widths (w_m) are compared with the theoretical values by Griem [1] (w_G) and by Dimitrijevic and Sahal-Brechot [2] (w_D). As it can be seen, there are no important discrepancies between different experimental results and in the comparison with theoretical values. The only exceptions are the results by Kusch [14] and Greig and Jones [13]. The discrepancy in Kusch's results may be attributed to a lack of control of the self-absorption. On the other hand, the result by Greig and Jones [13] at high density exhibits an important discrepancy, even though there are not too many experimental data at such high-electron densities to compare with. The reason for this discrepancy may be due to the fact that at high densities ($\geq 10^{17}$ cm^{-3}), the 5016-Å line is not an isolated one, on the contrary, it has a forbidden component (5042 Å) that appears as a result of the strong interaction of the upper level of the line with the $3\,^1D$ level [13]. The reason for the small disagreements between the other experimental results

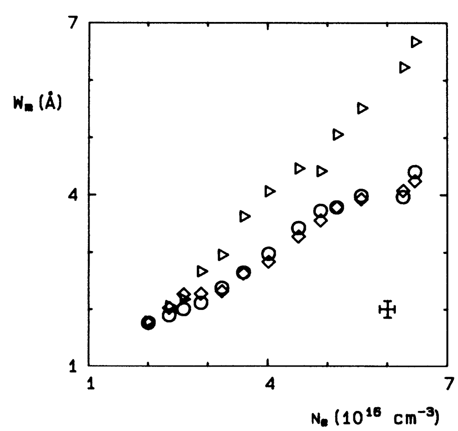

FIG. 4. Stark FWHM of the lines as a function of the electron density. ◇, 6678 Å; ○, 5016 Å; and ▷, 4713 Å. This figure includes the average errors bars of the quantities measured in the present work.

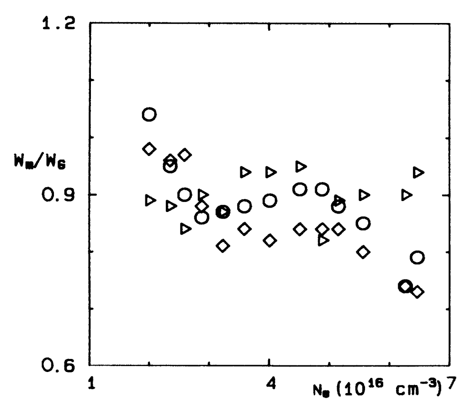

FIG. 6. The ratios (w_m/w_G) of the lines as a function of the electron density. ◇, 6678 Å; ○, 5016 Å; and ▷, 4713 Å.

TABLE II. Review of previous experimental results for the 5016-Å He I line.

Reference	N_e (10^{16} cm^{-3})	N_e determination	w_m/w_G	w_m/w_D	T (K)
Wulff [9]	3.2	Inglis-Teller	0.72	0.85	30 000
Berg [10]	16.5	H, He lines	0.86	1.01	24 000
Bötticher [11]	1.0–2.0	LTE	1.13–0.94	1.33–1.11	15 600–16 900
Lincke [12]	9.3	H, He lines	0.86	1.01	22 700
Greig [13]	2.7–17	H_β line	1.20–1.17	1.42–1.38	23 000–25 000
Kusch [14]	0.8–4.6	H_β line	1.66–1.86	1.96–2.19	18 000–26 000
Einfeld [15]	2.0–3.5	He continuum	0.99–0.97	2.01	38 000
Chiang [16]	10.5–12.6	Interferometry	1.01–0.88	1.19–1.04	17 400
Soltwisch [17]	6.7–7.7	Interferometry	0.91–0.96	1.07–1.13	20 000
Kelleher [18]	0.3–1.3	H_β line	0.92	1.09	20 900
This work	2.00–6.46	Interferometry	0.76–0.94	1.55–1.28	19 000–43 000

presented in Table II is not known.

A clearer comparison between all experimental results (listed in Table II) is given in Fig. 7. With the two exceptions mentioned above, this figure shows good agreement between all these data, and a similar situation is found for the other two spectral lines, even though there are not so many previous data.

Afterwards, we tried to find out a calibration relation for each line. This relation will be established between N_e and w_m, and according to Fig. 5 the temperature has also been included in this dependence. Then, for each line, we have plotted $\ln N_e$ vs $\ln w_m$, in these plots we have included all the experimental points, only in the case of the 5016-Å line we have excluded the two exceptions already mentioned. For the three lines we have found fits with prefactor of $\ln N_e$ very close to 1 (the differences with 1 may be due, according to Griem [1], to the fact that the relation w_m to N_e it is not strictly linear). The

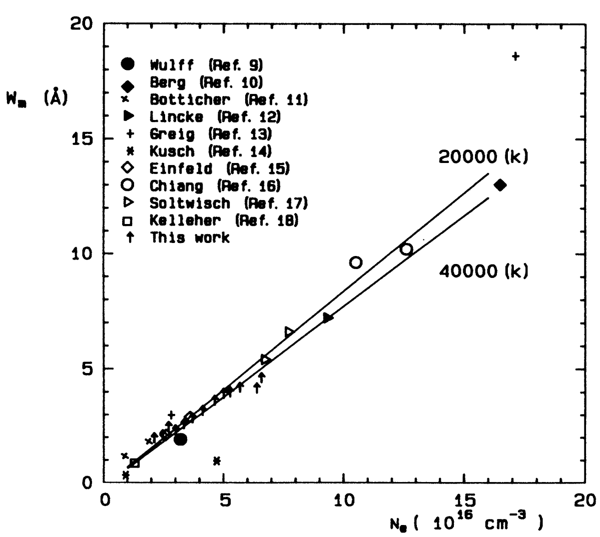

FIG. 7. Stark FWHM for the 5016-Å line as a function of the electron density and temperature; results from previous experimental work are included in this plot.

sign of the prefactor of $\ln T$ is, in agreement with theory, positive for the 4713-Å line, and negative for the other two. In the fits all the points have been weighted according to the accuracy criteria given by Konjevic and Roberts [19], our results have been considered as B.

For the 5016-Å He I line, the fit, which has been done in a range of electron density from 10^{16} to 16.5×10^{16} cm^{-3}, gives the following result:

$$\ln w(\text{Å}) = -38.99(\pm1.4) + 1.08(\pm0.02)\ln N_e(\text{cm}^{-3}) - 0.12(\pm0.04)\ln T\ (\text{K})\ .$$

In Fig. 7 we have plotted this function together with the experimental points. From all these results, it is reasonable to conclude that the accuracy of the electron densities determined from the FWHM of the 5016-Å line, used as a standard, should be about 15%.

For the He I line 6678 Å the same process has been followed. For this line there are only previous results in Refs. [18], [20], and [21]. With a fit (of the same kind) done with all the experimental points, we obtained the following relation:

$$\ln w(\text{Å}) = -34.90(\pm1.5) + 1.040(\pm0.014)\ln N_e(\text{cm}^{-3}) - 0.35(\pm0.04)\ln T\ (\text{K})$$

which has been obtained in the range of electron densities $(1.03-10)\times10^{16}$ cm^{-3}.

For the last of the three measured lines, 4713 Å, there are previous experimental results in Ref. [19], [10], [12], [18], and [22]. A similar fit, including all these data, gives the relation

$$\ln w(\text{Å}) = -39.97(\pm1.6) + 1.05(\pm0.02)\ln N_e(\text{cm}^{-3}) + 0.13(\pm0.05)\ln T\ (\text{K})$$

obtained in the interval of electron densities $(0.6-13)\times10^{16}$ cm^{-3}.

As the widths of these two isolated He I lines give electron densities that are consistent with the results given by the 5016-Å line, we will assign to them the same accuracy. As an alternative calibration for these three lines, we will suggest the theoretical values by Griem [1] multiplied by the mean values of the ratios w_m/w_G obtained in this work.

ACKNOWLEDGMENTS

The authors would like to thank Dr. M. A. Gigosos for his help and interest in this work, and also they would like to thank the Dirección General de Investigación Científica y Técnica (Ministerio de Educación y Ciencia) of Spain for its financial support under Contract No. PB87-0901.

[1] H. R. Griem, *Spectral Line Broadening by Plasmas,* (Academic, New York, 1974).

[2] M. S. Dimitrijevic and S. Sahal-Brechot, J. Quant. Spectrosc. Radiat. Transfer **31**, 301 (1984).

[3] I. Gonzálex, S. Mar, and V. Cardeñoso, Atti Fond. Giorgi Ronchi **41**, 501 (1986).

[4] M. I. González, M. C. Pérez, M. I. de la Rosa, and S. Mar, Jpn. J. Appl. Phys. **29**, 1189 (1990).

[5] M. I. de la Rosa, M. C. Pérez, A. M. de Frutos, and S. Mar, Phys. Rev. A **42**, 7389 (1990).

[6] W. L. Wiese, *Plasma Diagnostic Techniques,* edited by H. Huddlestone and S. L. Leonard (Academic, New York, 1965).

[7] C. Pérez, Ph.D. thesis, Universidad de Valladolid, 1990.

[8] J. T. Davies and J. M. Vaughan, Astrophys. J. **137**, 1302 (1963).

[9] H. Wulff, Z. Phys. **150**, 614 (1958).

[10] H. F. Berg, A. W. Ali, R. Lincke, and H. R. Griem, Phys. Rev. **125**, 1 (1962).

[11] W. Bötticher, O. Roder, and K. H. Wobig, Z. Phys. **175**, 480 (1963).

[12] R. Lincke, thesis, University of Maryland, 1964.

[13] J. R. Grieg and L. A. Jones, Phys. Rev. A **1**, 1261 (1970).

[14] H. J. Kusch, Z. Naturforsch. Teil A **26**, 1970 (1971).

[15] D. Einfeld and G. Sauerbrey, Z. Naturforsch. Teil A **31**, 310 (1976).

[16] W. T. Chiang, D. P. Murphy, Y. G. Chen, and H. R. Griem, Z. Naturforsch. Teil A **32**, 818 (1977).

[17] H. Soltwisch and J. Kusch, Z. Naturforsch. Teil A **34**, 300 (1979).

[18] D. E. Kelleher, J. Quant. Spectrosc. Radiat. Transfer **25**, 191 (1981).

[19] N. Konjevic and J. R. Roberts, J. Phys. Chem. Ref. Data **5**, 2 (1976).

[20] J. C. Gautier, J. P. Geindre, C. Goldbach, N. Grandjouan, A. Mazure, and G. Nollez, J. Phys. B **14**, 2099 (1981).

[21] B. T. Vujicic (unpublished).

[22] R. N. Morris and J. Cooper, Can. J. Phys. **51**, 1746 (1973).